

# On Nonlinear Filtering Using Two-Grid Coupled Cellular Neural Networks

Liviu Goras\*, Iulian Ciocoiu\*, Emilian David\*, Paul Ungureanu\*

**Abstract** - The behaviour of two-grid coupled Cellular Neural Networks (CNN's) able to exhibit Turing patterns is investigated for initial conditions representing human faces. Preliminary results based on filtering with various positions and widths of the band of unstable modes are presented. Experiments indicate that "Turing-faces" may represent a useful pre-processing technique that may increase the performance of traditional PCA-based face recognition approaches.

## 1 INTRODUCTION

Since their invention [1,2], CNN's have been thoroughly investigated for their applications in image processing. Inspired from biology, CNN's are homogeneous arrays of *identical and identically coupled* nonlinear dynamic cells. The image to be processed with an 2D N by M CNN is introduced through the input and/or the state of the cells, each cell corresponding to a pixel of the image. Two-port or even n-port cells can be used.

An interesting phenomenon, which has been shown to appear in CNN's, is that of pattern formation - a behaviour that seems not to have been yet enough exploited (*pattern* will be the name for any stable equilibrium point). Many connections with phenomena from other domains including biology have been made so far. Among them, pattern formation based on a mechanism similar to that proposed by Turing [3,4] to explain morphogenesis has been reported in two-grid coupled second order cell CNN's [5,6]. A CNN architecture capable to produce Turing patterns has been reported in [5] and is sketched in Fig. 1. It consists of second order two-port cells "sandwiched" between two resistive grids, each grid connecting similar ports.

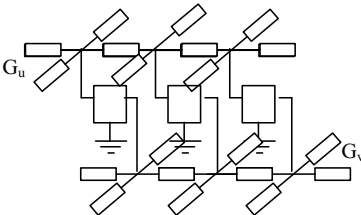


Fig. 1. Sketch of the two-grid architecture.

The analysis is greatly simplified if the nonlinearity of the cells is piecewise linear. A possible realization of the cells consisting of four linear elements including a voltage controlled current source and a nonlinear resistor is shown in Fig. 2. A cell is represented in Fig. 1 and is described by the equations:

$$\begin{aligned} i_1 &= f(u, v) = -Gu - f(u) + Gv \\ i_2 &= \tilde{g}(u, v) i_1 = (G - g)u - Gv \end{aligned} \quad (1)$$

where the \$f(u)\$ is the piecewise linear characteristic of the nonlinear resistor.

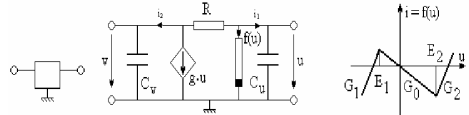


Fig. 2. Two-port cell and i-v characteristic of the piecewise nonlinear resistor.

In the general case, the behaviour of a 2D CNN composed of \$M \times N\$ cells is described by the following system of equations:

$$\begin{aligned} C_u \frac{du_{ij}(t)}{dt} &= f(u_{ij}, v_{ij}) + G_u \nabla^2 u_{ij} \\ C_v \frac{dv_{ij}(t)}{dt} &= \tilde{g}(u_{ij}, v_{ij}) + G_v \nabla^2 v_{ij} \\ i &= 0, \dots, M - 1, j = 0, \dots, N - 1 \end{aligned} \quad (2)$$

where: \$\nabla^2 x\_{ij} = x\_{(i+1)j} + x\_{(i-1)j} + x\_{i(j+1)} + x\_{i(j-1)} - 4x\_{ij}\$ is the Laplacean (which, for the 1-D case, has the form \$\nabla^2 x\_i = x\_{i+1} + x\_{i-1} - 2x\_i\$). With the notations:

$$\gamma = \frac{1}{C_u}; D_u = \frac{G_u}{C_u}; D_v = \frac{G_v}{C_v}; g(u_i, v_i) = \frac{C_u}{C_v} \tilde{g}(u_i, v_i) \quad (3)$$

the equations become:

$$\begin{aligned} \frac{du_{ij}(t)}{dt} &= \gamma f(u_{ij}, v_{ij}) + D_u \nabla^2 u_{ij} \\ \frac{dv_{ij}(t)}{dt} &= \gamma g(u_{ij}, v_{ij}) + D_v \nabla^2 v_{ij} \end{aligned} \quad (4)$$

Linearization of these equations gives:

\* „Gh. Asachi” Technical University, Faculty of Electronics and Telecommunications, Bd. Carol 11, Iasi 6600, Romania, e-mail: lgoras@etc.tuiasi.ro, iciocoiu@etc.tuiasi.ro, edavid@scs4.etc.tuiasi.ro, pungureanu@scs4.etc.tuiasi.ro.

$$\begin{aligned}\frac{du_{ij}(t)}{dt} &= \gamma(f_u u_{ij} + f_v v_{ij}) + D_u \nabla^2 u_{ij} \\ \frac{dv_{ij}(t)}{dt} &= \gamma(g_u u_{ij} + g_v v_{ij}) + D_v \nabla^2 v_{ij}\end{aligned}\quad (5)$$

where  $f_u, f_v, g_u, g_v$  are the elements of the Jacobian matrix of  $f(u, v)$  and  $g(u, v)$ ,  $D_u$  and  $D_v$  are the diffusion coefficients and  $\gamma$  is a scaling coefficient. For the cell in Fig. 2, the above equations are valid for u-voltages within the interval  $[E_1, E_2]$ . In this case, the relations between the Jacobian parameters and the circuit elements are:

$$f_u = -(G + G_t), \quad f_v = G, \quad g_u = \frac{C_u}{C_v}(G - g), \quad g_v = \frac{C_u}{C_v}G \quad (6)$$

In the case when all cell voltages are in the central linear part of the nonlinear characteristics the analysis simplifies considerably due to linearity and symmetry (which is valid until at least one cell reaches saturation). In such cases the dynamics can be easily studied using the decoupling technique, which consists of a change of variable based on a set of spatial orthogonal functions.

Using the notations from [6], we transform the system of equations by means of the change of variables:

$$\begin{aligned}u_{ij}(t) &= \sum_{m=0, n=0}^{M-1, N-1} \Phi_{MN}(i, j, m, n) \hat{u}_{mn}(t) \\ v_{ij}(t) &= \sum_{m=0, n=0}^{M-1, N-1} \Phi_{MN}(i, j, m, n) \hat{v}_{m, n}(t)\end{aligned}\quad (8)$$

$m=0, 1, \dots, M-1, n=0, 1, \dots, N-1$

where  $\Phi_{MN}(i, j, m, n)$  are eigenfunctions (dependent on the boundary conditions) of the 2D Laplacean i.e.,  $\nabla^2 \Phi_{MN}(i, j, m, n) = -k_{mn}^2 \Phi_{MN}(i, j, m, n)$  and  $-k_{mn}^2$  are the eigenvalues, proportional to a sum of squares of sine functions.

With the above change of variable and taking the scalar product of both the resulted equations, the dynamics of the CNN is described by the following set of pairs of *decoupled* linear equations

$$\begin{bmatrix} \dot{\hat{u}}_{mn} \\ \dot{\hat{v}}_{mn} \end{bmatrix} = \left( \gamma \begin{bmatrix} f_u & f_v \\ g_u & g_v \end{bmatrix} - k_{mn}^2 \begin{bmatrix} D_u & 0 \\ 0 & D_v \end{bmatrix} \right) \begin{bmatrix} \hat{u}_{mn} \\ \hat{v}_{mn} \end{bmatrix} \quad (9)$$

Thus, the set of  $2 \times M \times N$  coupled differential equations in the u and v variables transforms into  $M \times N$  sets of pairs of second order differential equations in the new variables - the amplitudes of the spatial components of the voltages.

The natural frequencies,  $\lambda_{mn1}$  and  $\lambda_{mn2}$  are the roots of the characteristic polynomials

$$\begin{aligned}\lambda_{mn}^2 + \lambda_{mn} [k_{mn}^2 (D_u + D_v) - \gamma(f_u + g_v)] + D_u D_v k_{mn}^4 - \\ - \gamma(D_v f_u + D_u g_v) k_{mn}^2 + (f_u g_v - f_v g_u) = 0\end{aligned}\quad (10)$$

The dynamics of the CNN is significantly determined by the roots of the characteristic equations, even though the results are valid only for the linear central part. The crucial aspect regarding pattern formation is that, in certain conditions, at least one of the roots of the characteristic equation has positive real part. This will cause the corresponding spatial mode(s) to grow until some nonlinearity will limit the growth. The *dispersion surface* represents the real part of the temporal eigenvalues versus the spatial eigenvalues.

$$\begin{aligned}\text{Re } \lambda_{1,2}(k_{mn}^2) = \text{Re } \left\{ \gamma \frac{f_u + g_v}{2} - k_{mn}^2 \frac{D_u + D_v}{2} + \right. \\ \left. + \sqrt{\left[ \gamma \frac{(g_v - f_u) + k_{mn}^2 (D_u - D_v)}{2} \right]^2 + \gamma^2 f_v g_u} \right\}\end{aligned}\quad (11)$$

In principle, a pattern, i.e., a stable equilibrium points towards which the network emerges, can develop when the characteristic equation has at least one root with positive real part corresponding to a *nonzero* spatial frequency. Indeed, the instability of the zero spatial frequency spatial mode will determine that *all* cell go to either a positive or negative saturation value or simultaneously oscillate - situations that will not be considered to yield patterns. An interesting situation appears when the origin is a **stable** equilibrium point for an isolated cell and an **unstable** equilibrium point for the whole array. The necessary conditions (Turing) that ensure the *instability* of an array built of *stable* cells linked together through resistive grids are [5, 6]:

$$\begin{aligned}f_u + g_v &< 0 \\ f_u g_v - f_v g_u &> 0 \\ D_v f_u + D_u g_v &> 0 \\ (D_v f_u - D_u g_v)^2 + 4 D_u D_v f_v g_u &> 0\end{aligned}\quad (12)$$

It has been shown that the results of the linear theory fit remarkably well with the simulations especially for 1D arrays, which means that the nonlinearity plays mainly the role of limiting the growing process of the unstable spatial modes. In the 2D case, however, the linear theory is able to predict the final pattern in fewer cases.

## 2 NONLINEAR FILTERING OF FACES

Face recognition has represented for more than one decade one of the most active research areas in pattern recognition. A plethora of approaches have been proposed and evaluation standards have been defined, but current state-of-the-art solutions still need to be improved in order to cope with the

recognition rates and robustness requirements of commercial products. Most of the approaches may be classified into two categories: a) geometric feature-based techniques, relying on the identification of specific components of a face such as eyes, nose, mouth, and distances among them; b) holistic template-based techniques, usually based on projecting the original (high-dimensional) images onto lower dimensional subspaces spanned by specific basis vectors. Eigenfaces [7] represent a *de facto* standard for the second approach and, although superior solutions exist, still defines a performance reference against which any new method is compared. A pattern recognition system includes three modules, *i.e.* the preprocessing stage, the feature extraction, and the classification stage. Several distinct preprocessing techniques are currently used, including both common image processing techniques such as histogram normalization or edge detection, and more face-oriented approaches like projection-combined principal components analysis ((PC)<sup>2</sup>A) [8], and eigenhills [9]. We propose the use of two-grid coupled CNN's as a novel preprocessor: original face images will act as initial states to the system, and the final pattern will represent a nonlinearly filtered version of the images. Several distinct paths have been preliminarily investigated using the images available in the Olivetti database (it contains 10 images for 40 persons, and includes variations in pose, light conditions, scaling, and expression; dimension is 112x92 pixels):

A) obtain Turing-patterns using CNN's with various dispersion surfaces for each downsampled image in the database and identify the closest neighbors for each person, using classic distance measures

B) perform a multiresolution decomposition of the original images based on the Discrete Wavelet Transform (DWT) and keep only the low-frequency components. Besides dimensionality reduction (in our case the resulting images become 28x28 pixels), this procedure is known to offer face expression invariance. Obtain low-resolution Turing-faces and compare them using the same distance measures.

C) obtain low-resolution face images using DWT and perform PCA decomposition (basically, PCA is a linear projection technique on a subspace spanned by the principal eigenvectors of the input covariance matrix. When applied to face processing, those basis vectors are called eigenfaces and define the directions along which the variance of the original images is maximized). We then reconstruct an approximative version of the original images based on the most expressive eigenvectors (those corresponding to the largest eigenvalues of the image covariance matrix). Obtain Turing-patterns using the

approximated images as initial conditions, and compare them.

D) detect edges of the original images, then use them as initial conditions to the CNN's in order to obtain Turing patterns.

Examples for each of the cases above are presented in Fig. 4-7. The CNN parameters used for the tests are  $f_u = 0.1$ ,  $f_v = -1$ ,  $g_u = 0.1$ ,  $g_v = -0.2$ ,  $D_u = 1$  and  $D_v$ ,  $\gamma$  are chosen to select different bands of unstable modes used in simulations. The dispersion surfaces for 4 different bands of unstable modes are given in Fig. 3.

### 3 EXPERIMENTAL RESULTS

In Fig. 4 Turing patterns obtained for initial conditions given by low resolution versions of the original images for 2 different persons and for the 4 bands of unstable modes are presented. Fig. 5 represents Turing patterns obtained from low frequency components of DWT of original images and Fig. 6 from initial conditions given by their approximations using PCA decomposition and selection of most significant eigenvectors. In Fig. 7 comparative results for using the original and corresponding edge images (at high resolution) as initial conditions are given.

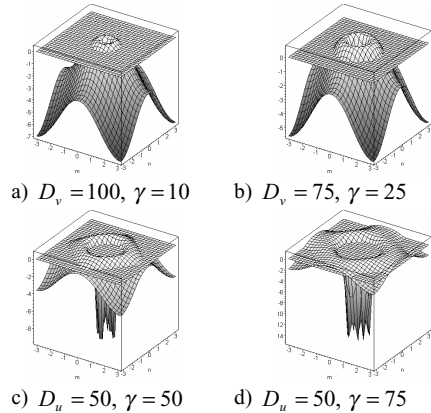


Fig. 3: Dispersion surfaces

Similarity analysis based on L2 distance between Turing patterns belonging to 2 distinct persons revealed that these are more similar than the original images, especially for the approach including PCA decomposition.

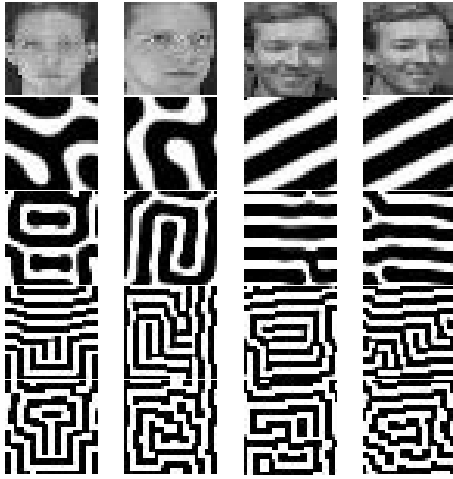


Fig. 4: Downsampled original images as initial conditions and resulting Turing patterns

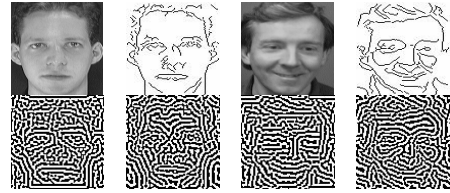


Fig. 7: Edges of original images as initial conditions and resulting patterns

#### 4 CONCLUSIONS

The use of 2-layer CNN's as a pre-processor in face recognition applications has been investigated. The method provides stable patterns from which feature extraction may be performed. The preliminary results obtained so far show that the above processing may represent an interesting complementary tool in face recognition.

#### Acknowledgments

This work was partly supported by the Swiss National Science Foundation under Grant SCOPES 7RUPJ062381.

#### References

- [1] L. O. Chua, L. Yang, "Cellular Neural Networks: Theory", IEEE Trans. Circuits Syst., vol. 35, no 10, pp. 1257-1272, October 1988.
- [2] L. O. Chua, L. Yang, "Cellular Neural Networks: Applications", IEEE Trans. Circuits Syst., vol. 35, no 10, pp 1273-1290, October 1988.
- [3] A. M. Turing, "The Chemical Basis of Morphogenesis", Phil. Trans. Roy. Soc. Lond. B 237, pp.37-72, October 1952.
- [4] J. D. Murray, *Mathematical Biology*, Springer-Verlag, Berlin Heidelberg, 1993.
- [5] L. Goras, L. O. Chua, D. M. W. Leenaerts, "Turing Patterns in CNN's-Part I: Once Over Lightly", IEEE Trans. Circuits Syst, vol.42, pp. 602-611, October 1995.
- [6] L. Goras, L. O. Chua, "Turing Patterns in CNN's - Part II: Equations and Behaviors", IEEE Trans. Circuits Syst, vol.42, pp. 612-626, October 1995.
- [7] M. Turk, and A.P. Pentland, "Eigenfaces for recognition", *J. of Cognitive Neuroscience*, vol. 3, no. 1, pp. 71-86, 1991
- [8] J. Wu, and Z.H. Zhou, "Face recognition with one training image per person", *Pattern Recognition Letters*, vol. 23, pp. 1711-1719, 2002
- [9] A. Yilmaz, M. Gokmen, "Eigenhill vs. eigenface and eigenedge", *Pattern Recognition*, vol. 34, pp. 181-184, 2000

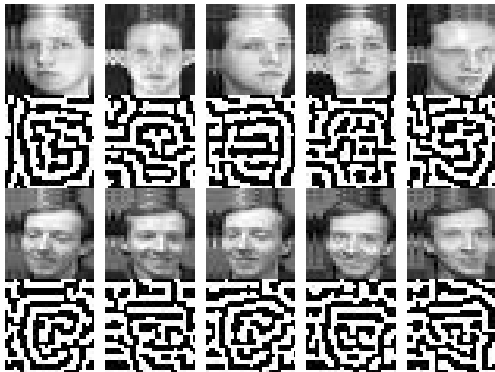


Fig.5: Downsampled images based on DWT as initial conditions and resulting patterns

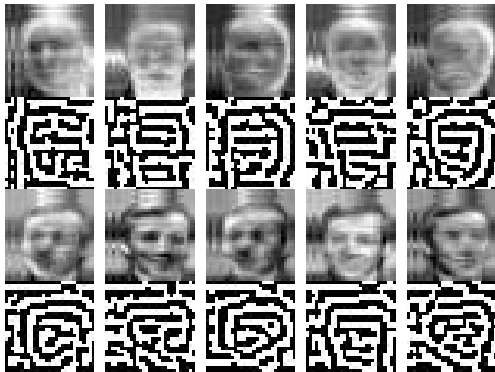


Fig. 6: PCA-based approximations of downsampled images as initial conditions and resulting patterns